Water Science & Technology

Water Science & Technology Vol 88 No 11, 2707 doi: 10.2166/wst.2023.361

Full dynamic control of dairy wastewater treatment by aerobic granular sludge using electric conductivity and oxygen uptake rate

Flinn De Vleeschauwer and Jan Dries *

Research Group BioWAVE, Biochemical Wastewater Valorisation and Engineering, Faculty of Applied Engineering, University of Antwerp, Groenenborgerlaan 171, Antwerp 2020, Belgium
*Corresponding author. E-mail: jan.dries2@uantwerpen.be

JD, 0000-0002-0204-5697

ABSTRACT

The objective of the current study was to determine the applicability of a sensor-based dynamic control strategy for the treatment of real variable dairy wastewater by aerobic granular sludge (AGS) performing enhanced biological phosphorus removal (EBPR). Two parallel sequencing batch reactors (SBRs) were set up that used only an anaerobic feast/aerobic famine microbial selection strategy to successfully obtain sludge granulation. SBR-STA used a fixed cycle length, while the duration of the reaction steps in SBR-DYN was variable. The control strategy was based solely on (derived) signals from low-cost and common sensors. The profile of the electric conductivity during the anaerobic reaction step was related to the microbial release of phosphate (PO_4-P) and the associated uptake of dissolved organic carbon (DOC) by polyphosphate-accumulating organisms (PAOs). Control of the aerobic reaction step was based on the oxygen uptake rate (OUR). This resulted in a dynamic reactor operation with significant efficiency gains, such as 32% shorter cycle times and 42% higher sludge loading rates without impairing the effluent quality. These results extend the existing potential of indirect control strategies to full biological nutrient removal processes, which may be of great assistance to the operators and designers of industrial installations.

Key words: enhanced biological phosphorus removal (EBPR), glycogen-accumulating organisms (GAOs), indirect control strategies, industrial wastewater, microbial selection, polyphosphate-accumulating organisms (PAOs)

HIGHLIGHTS

- Aerobic granulation was achieved by an anaerobic feast/aerobic famine operation in sequencing batch reactors treating real dairy wastewater.
- Enhanced biological phosphorus removal (EBPR) was stable and efficient.
- The duration of the reaction steps could be controlled using electric conductivity and oxygen uptake rate.
- Significant efficiency gains can be reached by using dynamic control strategies in the operation of AGS systems.

INTRODUCTION

Within the food industry, the dairy sector is one of the largest producers of industrial wastewater in Europe (Kolev Slavov 2017). On average, the industry produces 2.5 times more wastewater than dairy products. Biological processes represent a central step in dairy wastewater treatment, which could be further optimized by adopting the novel aerobic granular sludge (AGS) technology (Schwarzenbeck *et al.* 2005; Wichern *et al.* 2008; Silva *et al.* 2023). AGS relies on the formation of microbial self-immobilized aggregates, resulting in a very compact and dense structure. Therefore, it has better settleability, larger biomass concentration, higher resilience to toxicity, capability to operate at higher organic and shock-loading rates, and the possibility to biodegrade organic carbon and remove nutrients simultaneously, with less sludge production and a lower footprint (Campo *et al.* 2020). Although there is still debate on which factor is the key driver for stable granulation, de Kreuk & van Loosdrecht (2004) showed the decisive role of slow-growing organisms and more specifically of phosphate (PAO) and glycogen (GAO)-accumulating organisms. The selection of GAO and PAO, through an anaerobic feast/aerobic famine regime, leads to the formation of dense granular sludge, because the uptake and conversion rate of the substrates by the granules is lower than the transport rate into the granules (van Dijk *et al.* 2022). Other researchers stress the importance of a

hydraulic (settling) pressure to get rid of the bad settling floccular sludge fraction, while critical organic loading rates, shear stress, and so on, have all been proposed as equally relevant (e.g. Franca *et al.* 2018). Furthermore, AGS produces a valuable gel-forming biopolymer referred to as alginate-like extracellular polysaccharides (ALE), responsible for the strength, elasticity, and hydrophobicity of AGS (Schambeck *et al.* 2020).

PAOs act in the enhanced biological phosphorus removal (EBPR) process, operated under alternating anaerobic and aerobic conditions. Under anaerobic feast conditions, PAOs use the energy from hydrolyzing phosphodiester bonds of stored polyphosphates to convert and store volatile fatty acids (VFAs) as polyhydroxyalkanoates (PHAs). In this phase, PAOs release the orthophosphate (PO_4-P) in the bulk liquid (Izadi *et al.* 2020). Under aerobic famine conditions, the stored PHA is oxidized, and the energy released is mainly used for biomass production, PO_4-P absorption, and polyphosphate synthesis. More PO_4-P is absorbed in the aerobic step than released in the anaerobic step, leading to a net decrease in the liquid PO_4-P concentration. GAOs, on the other hand, have a similar metabolism, i.e. VFA conversion to PHA under anaerobic feast conditions followed by PHA oxidation under aerobic famine conditions, but without the associated P cycling.

EBPR is a promising process for treating the PO_4-P-rich dairy wastewater, with P concentrations 5–20 times higher than in municipal wastewater (Kushwaha *et al.* 2011). An efficient EBPR process could meet stringent effluent qualities (1–2 mg P L^{-1}) if a careful design and operation are practiced (Ahn & Park 2008). Industrial application of EBPR however is not widespread. A recent survey among 90 of the 354 industrial biological wastewater treatment plants in Flanders showed that, of the 39 companies requiring P removal, none applied EBPR but instead removed P by precipitation after chemical treatment with ferric iron chloride or poly aluminium chloride (Cornelissen *et al.* 2018). Possible reasons are the perceived complexity and the lack of knowledge of the EBPR process, the ease of the chemical alternative, and the low cost of chemicals. A specific concern with the EBPR process is how it handles wastewater variability, which could be addressed by implementing a dynamic control strategy that measures the variability in wastewater composition and adjusts the operation of the treatment accordingly. While specific nutrient analysers and sensors are available on the market today, they require high investment and maintenance costs (Olsson 2012; Zhang *et al.* 2022). As a result, they are barely applied in industry (Cornelissen *et al.* 2018). An alternative approach is the use of low-cost and robust indirect sensors. Control strategies for biological nitrogen (N) removal using pH, redox potential, and dissolved oxygen (DO) sensors have been developed and extensively tested (e.g. Yang *et al.* 2010; Ribeiro *et al.* 2017), but much less so for P removal. In EBPR systems, conductivity sensors could be used, as changes in the conductivity are strongly related to the dynamics of PO_4-P uptake and release. In the anaerobic step, the conductivity increases because of the release of PO_4-P ions in the bulk liquid (Maurer & Gujer 1995). The conductivity profile can thus be used to dynamically control the anaerobic step in an EBPR AGS system. Short-term studies showed stable N and P removal by AGS with varying influent concentrations (Kishida *et al.* 2008). Long-term studies have verified the effectiveness of conductivity-based control while treating P-rich synthetic wastewater with variable composition (De Vleeschauwer *et al.* 2019). To the best of our knowledge, no industrial application of a conductivity-based dynamic control has been reported.

The objectives of this study are therefore to determine the applicability and effectiveness of a sensor-based dynamic control strategy for an EBPR AGS reactor treating real variable dairy wastewater.

MATERIALS AND METHODS

Reactor set-up and operation

Two parallel AGS SBRs were operated using an anaerobic/aerobic reaction sequence for 92 days. SBR-STA was operated statically with a fixed length of the different steps in the SBR cycle. SBR-DYN, on the other hand, was operated dynamically using conductivity-based dynamic control to adapt the length of the anaerobic step, and oxygen uptake rate (OUR) based control to adapt the length of the aerobic step. The reactors were seeded with activated sludge from a local sewage treatment plant with confirmed EBPR activity (Dockx *et al.* 2021). The sludge retention time in both reactors was kept at 30 days throughout the study.

The reactors were operated with a custom-built National Instruments LabVIEW® program, a Siemens PLC, and a Phoenix IO. The reactor operation (Figure 1) involved eight steps: unaerated mixing (10 min); pulse feeding of influent under anaerobic mixing conditions (flow dependent, but less than 1 min); anaerobic reaction (90 min for SBR-STA and dynamic for SBR-DYN); aerobic reaction (175 min for SBR-STA and dynamic for SBR-DYN); post-anoxic mixing (60 min); aerobic refresh (10 min); sludge settling (10 min); and discharge (5 min). The total cycle duration of SBR-STA was 360 min.

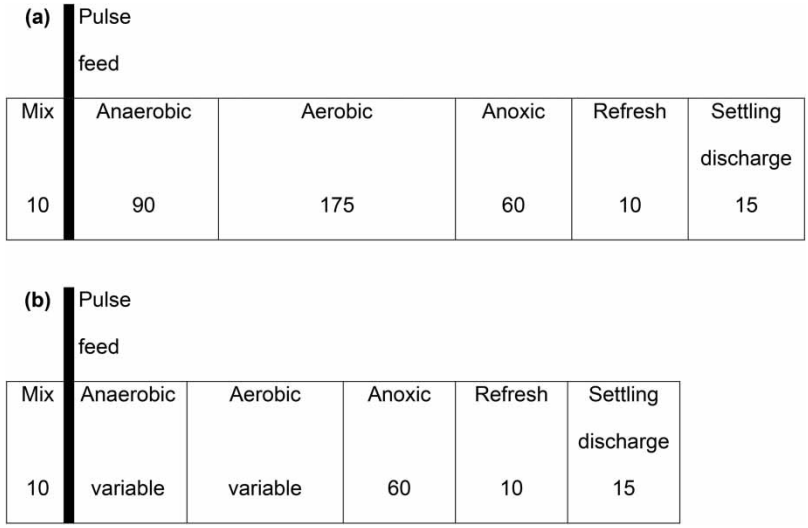

Figure 1 | SBR cycle times (in min) in SBR-STA (a) and SBR-DYN (b).

The reactors had a diameter of 24 cm and a height of 40 cm, corresponding to a height to diameter ratio (H/D) of 1.66. The volume exchange rate (VER) was 8%, with a working volume of 12.6 L and an influent volume per cycle of 1 L. The reactor was equipped with a peristaltic pump for influent feeding (Watson Marlow®), a mixer (Heidolph® RZR2020), a discharge valve (Eriks RX ER10.X33.S00), and an aeration system consisting of an aeration pump (koi flow 60, Aquadistri China®) and a 13 cm aeration disc (Aquadistri China®). Furthermore, the reactors were equipped with a luminescent dissolved oxygen (LDO) sensor (Hang Lange®) and a conductivity sensor (Hang Lange®). The DO concentration in the aerobic step was controlled using an on/off aeration control strategy. The aeration pump was activated when the DO concentration decreased below 1 mg L^{-1} and deactivated when the concentration increased above 2 mg L^{-1}. This aeration control allowed for the calculation of the OUR, as described by Dobbeleers *et al.* (2017). All sensor values were logged, and archived at the end of each cycle.

Composition of the industrial wastewater

The wastewater originated from a local full-scale plant treating dairy wastewater. The wastewater treatment consists of chemically enhanced primary treatment, using ferric chloride, in a dissolved air flotation unit to remove suspended solids and P, followed by a conventional activated sludge plant performing biological carbon and N removal. The raw wastewater was collected before the DAF unit, on a weekly basis, and kept in a fridge at 4 °C to minimize degradation. Before use, the wastewater was chemically pre-treated using ferric chloride (at 100 mg L^{-1} Fe) to remove the suspended solids (De Vleeschauwer *et al.* 2021). The average total and filtered chemical oxygen demand (COD) and suspended solids concentration in the raw wastewater were 2,158 $\pm$ 714 mg L^{-1}, 1,096 $\pm$ 515 mg L^{-1}, and 792 $\pm$ 300 mg L^{-1}, respectively. The variable composition of the wastewater, after pre-treatment, is shown in Table 1. Note that PO_4-P was added to the chemically pre-treated influent to reflect the average concentration in the raw influent.

Dynamic control of the duration of the anaerobic and aerobic steps

The control of the anaerobic step duration is based on the conductivity profile (Maurer & Gujer 1995). The control strategy applied in the current study was developed for synthetic wastewater by De Vleeschauwer *et al.* (2019) and was based on the slope of the conductivity profile. The control strategy used four calculation variables (CVs). CV1 and CV2 are the time intervals between consecutive sensor values and the number of sensor values per slope calculation, respectively. The cut-off point is determined by a minimal slope (CV3) and the number of slopes (CV4) that meet the cut-off requirements. In total, the control strategy runs through three loops to dynamically control the duration of the anaerobic step (Figure 2).

CV1, CV2, and CV4 were 20 s, 30, and 30, respectively. The slope setpoint CV3 needed to be adjusted regularly to achieve effective endpoint detection, probably due to the variable composition of the industrial wastewater. CV3 varied between 0.8 and 3 mS (cm d)$^{-1}$.

Table 1 | Composition of the chemically pre-treated dairy wastewater fed to the AGS reactors (14 different batches)

Parameter (unit)	Min	Max	Avg ± SD	%CV
Total COD (mg L^{-1})	268	1,590	795 ± 368	46
Filtered COD (mg L^{-1})	180	1,498	735 ± 378	51
PO_4-P (mg L^{-1})	9.4	14.5	10.8 ± 1.2	11
NH_4-N (mg L^{-1})	21.7	84	46.4 ± 15.6	34
COD/P (–)	27	151	75 ± 31	41
COD/N (–)	8.3	35.5	18.4 ± 8.0	44

The aerobic step in SBR-DYN was controlled dynamically based on the OUR value. When three consecutive OUR values were below a biomass-specific OUR (sOUR) of 2 mg $(g_{MLVSS}\,h)^{-1}$, the aerobic step was terminated (De Vleeschauwer *et al.* 2019).

Analyses

COD, PO_4-P, NH_4-N, NO_3-N, and dissolved organic carbon (DOC) were analysed using standard methods, as described by De Vleeschauwer *et al.* (2019). All the analyses except total COD were performed on prefiltered samples (VWR® glass microfibers filter 693, particle retention: 1.2). The mixed liquor suspended solids concentration (MLSS), the mixed liquor volatile suspended solids concentration (MLVSS), and the sludge volume index (SVI) were measured according to the standard methods (APHA 1998). The sludge particle size distribution (DV10, DV50, and DV90) was measured with a Malvern Mastersizer 3000, as described by Caluwé *et al.* (2017).

The alginate-like extracellular polymer (ALE) content was measured by extracting the ALE at high temperature (80 °C) in a sodium carbonate solution (Na_2CO_3) (Felz *et al.* 2016). Sludge sampled from the reactors at the end of a cycle was centrifuged at 3,500 rotations per minute (rpm) for 10 min. Approximately 3 g of centrifuged sludge was resuspended in a sodium carbonate solution (0.5% w/v Na_2CO_3) and mixed at 400 rpm and 80 °C for 35 min. Afterwards, the mixture was centrifuged, and the supernatant, with the dissolved ALE, was collected. The pH of the supernatant was then adjusted to 2.2 ± 0.05 using a 1 M HCl solution to obtain the ALE in its acidic form. The solution was centrifuged, and the pellet, which is ALE in its acidic form, was retained. The pellet was then resuspended in demineralized water and centrifuged twice to remove any ions. Finally, the pellet was dried overnight at 105 °C and weighed.

In-situ measurements

Periodic *in-situ* measurements were carried out to measure the anaerobic DOC uptake efficiency. Samples were taken from the reactor at fixed time intervals and filtered. The DOC of the filtered samples was analysed. The anaerobic DOC uptake efficiency at any time (*ti*) was calculated with Equation (1):

$$\text{Anaerobic DOC uptake}(\%)\text{ at } ti = 100 \times \frac{\text{DOC}_{(\text{after feeding})} - \text{DOC}_{(ti)}}{\text{DOC}_{(\text{after feeding})} - \text{DOC}_{(\text{end})}} \quad (1)$$

where $DOC_{(after\ feeding)}$ is the DOC value in the reactor after the pulse feed step and $DOC_{(end)}$ is the DOC value at the end of the cycle.

RESULTS AND DISCUSSION

De Vleeschauwer *et al.* (2019) reported the successful application of a sensor-based control strategy to adapt the length of the anaerobic and aerobic reaction steps in an AGS SBR treating P-rich synthetic wastewater with COD/P values ranging from 21 to 116. This study investigated the applicability of this control strategy when treating real industrial wastewater from the dairy industry with variable COD content and COD/P ratios ranging from 27 to 151 (Table 1).

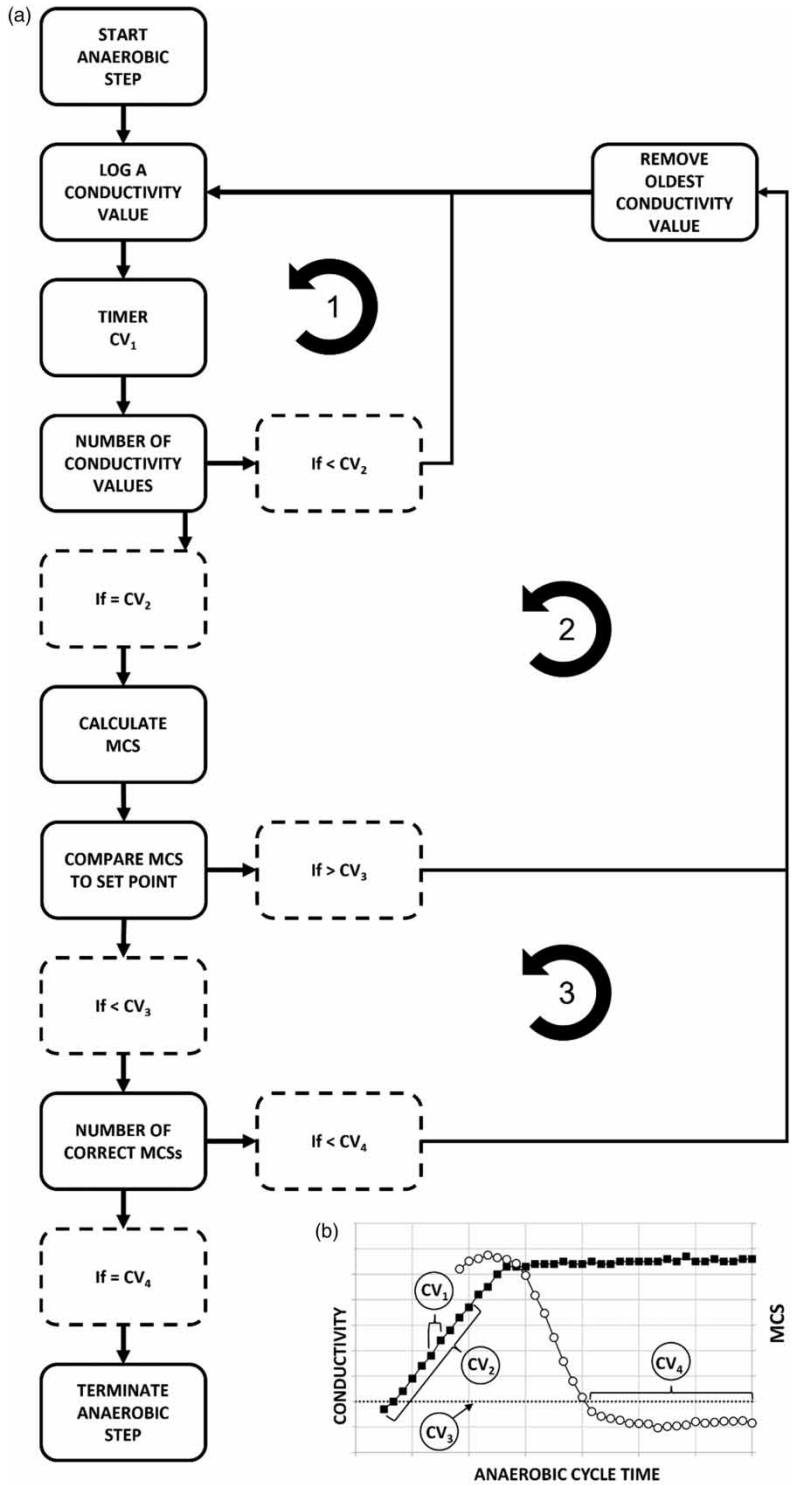

Figure 2 | (a) Schematic overview of the strategy used to dynamically control the length of the anaerobic reaction step, consisting of three loops; Loop 1, intermittent logging (every CV1 seconds) of paired conductivity and timestamp values, and building conductivity and time-stamp arrays (until the number of pairs in the array reaches a setpoint value CV2); Loop 2, the calculation (every CV1 seconds) of the moving conductivity slope (MCS) and comparing the MCS to the MCS setpoint CV3 (until the calculated MCS is lower than the MCS setpoint CV3); Loop 3, comparing the number of MCS that are smaller than CV3 to a setpoint amount (CV4), when the number of correct MCS equals the amount setpoint CV4, the anaerobic reaction step is terminated. (b) The conductivity and MCS profiles during the anaerobic reaction step of AGS reactor operation, (○) MCS, (■) conductivity (De Vleeschauwer *et al.* 2019).

Application of the dynamic control strategy

The focus in this section will be on the dynamic control of the anaerobic reaction step based on the conductivity profile. From the start of the operation, a clear relation between the conductivity profile and the evolution in the PO_4-P and DOC concentrations was observed in both reactors. The conductivity rapidly increased during the release of PO_4-P and the associated DOC uptake, and slightly levelled off when the liquid PO_4-P and DOC concentrations stabilized (Figure 3(a)).

The changes in the conductivity profile were better detected by using the MCS that showed a low and constant value when PO_4-P release and DOC uptake were finished (Figure 3(b)). The increase in conductivity is associated with the release of PO_4-P and the additional release of potassium and magnesium ions (Aguado *et al.* 2006). In studies using synthetic wastewater, a clear break in the conductivity profile and a sharp drop in the MCS are observed at the end of PO_4-P release, which is related to the complete uptake of the simple carbon substrate applied, mostly acetate or propionate only (e.g. Kishida *et al.* 2008; Weissbrodt *et al.* 2014; De Vleeschauwer *et al.* 2019). In contrast, in the present study, we observed a more gradual change in the conductivity and MCS profiles (Figure 3(a) and 3(b)) which is probably related to the more complex

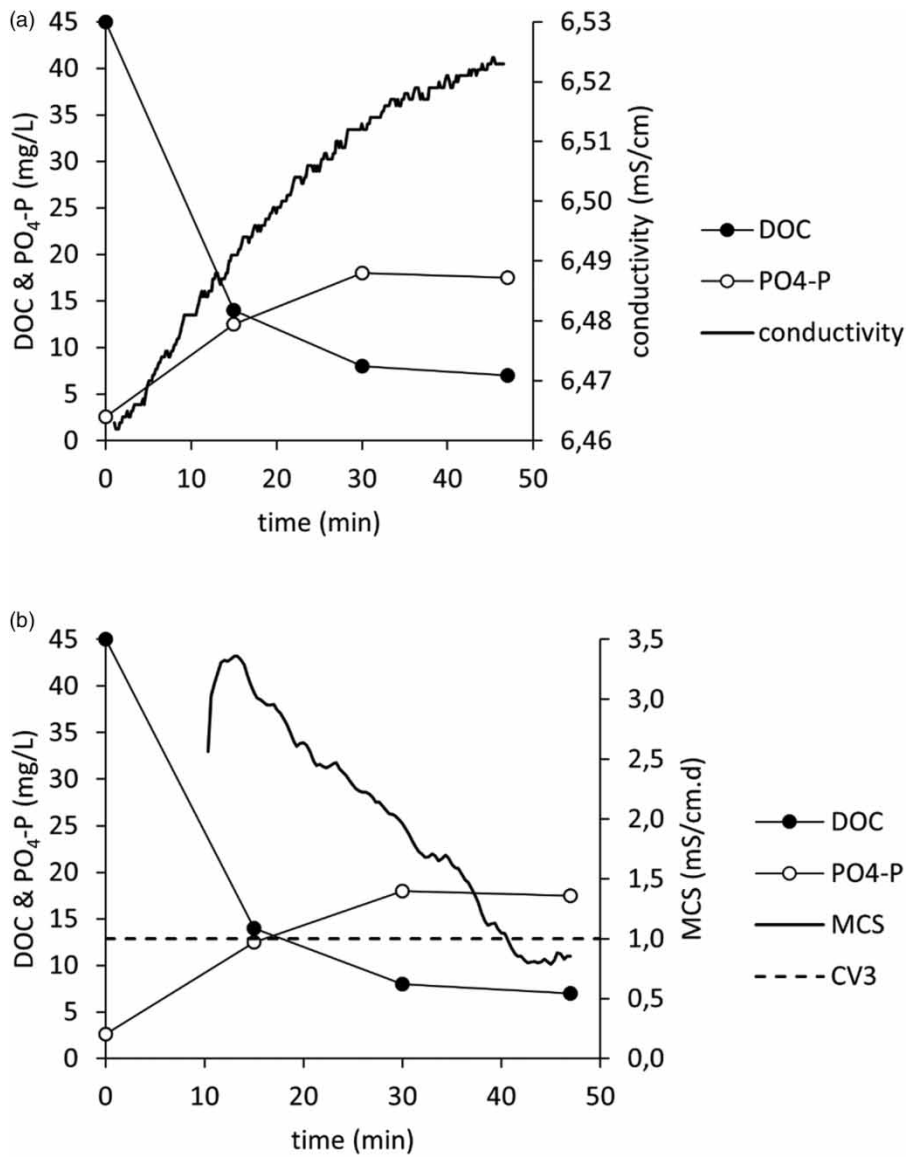

Figure 3 | Typical evolution of the DOC and PO_4-P concentrations and the conductivity sensor value (a), the MCS and CV3 (the MCS setpoint) (b) during the anaerobic step in SBR-DYN.

composition of the real dairy wastewater (Meunier *et al.* 2016). In addition, the value for CV3, which is the MCS setpoint (Figure 2), had to be regularly adjusted to allow successful endpoint detection when a new influent batch was treated. This was not the case when treating VFA-based synthetic influent even when the COD and PO_4-P concentrations varied significantly (De Vleeschauwer *et al.* 2019). In future research, more robust endpoint detection methods could be explored e.g. methods that are based on pattern recognition rather than on absolute setpoints to avoid this issue (e.g. Marsili-Libelli 2006).

The dynamic control of the aerobic reaction step, based on the OUR, is considered an established method and will not be discussed in detail. In brief, the aerobic reaction step was successfully terminated when three consecutive sOUR values were recorded below an endogenous respiration threshold value of 2 mg $(g_{MLVSS}\ h)^{-1}$ as extensively described in earlier research (e.g. Dries 2016; De Vleeschauwer *et al.* 2019, 2021).

Impact of the dynamic control strategy

In SBR-STA, the duration of the anaerobic and aerobic reaction steps was fixed at 90 and 175 min, respectively (Figure 1). In SBR-DYN, the duration of the anaerobic and aerobic reaction steps was not fixed, but dynamically adapted based on the MCS and the OUR. Figure 4 shows the impact of the dynamic control strategy on the duration of the anaerobic and aerobic reaction steps, as a function of the variable influent COD concentration.

The correlation between the duration of the anaerobic and aerobic steps and the influent COD concentration was statistically significant (Figure 4; $p < 0.0005$) indicating that the variation in the influent COD significantly contributes to the variation in the duration of both steps. This is explained by the specific metabolism of PAO in an EBPR system, where the uptake of COD from the liquid phase (and the subsequent intra-cellular storage) is driven by the release of PO_4-P which, in turn, is related to the conductivity profile. The close relation between COD uptake and PO_4-P release is expressed in the typical molar PO_4-P release to carbon uptake ratio of about 0.5 Pmol $Cmol^{-1}$ recorded in PAO-enriched systems fed with VFAs (Diaz *et al.* 2022). The dynamic control strategy thus ensures that all the assimilable carbon is taken up by PAO and/or GAO during the anaerobic reaction step, and prevents leakage of COD to the subsequent aerobic phase. The average DOC uptake during the anaerobic reaction step was 94 ± 4 and 92 ± 5% in SBR-DYN and SBR-STA, respectively. These uptake values are in the same range as previously observed in AGS systems fed with VFAs (De Vleeschauwer *et al.* 2019; Dockx *et al.* 2021). The near-complete substrate uptake during the anaerobic step promotes PAO (or GAO) over ordinary heterotrophic organisms and filamentous bacteria, and is key to the microbial selection strategy applied for granulation (Haaksman *et al.* 2020, 2023).

In SBR-DYN, the duration of the anaerobic reaction step varied from 25 to 56 min, with an average duration of 40 ± 10 min (Figure 4). The duration of the aerobic reaction step varied between 47 and 192 min, with an average duration of 109 ± 44 min. As a result, the total cycle also varied, between 176 and 337 min, with an average duration of 244 ±

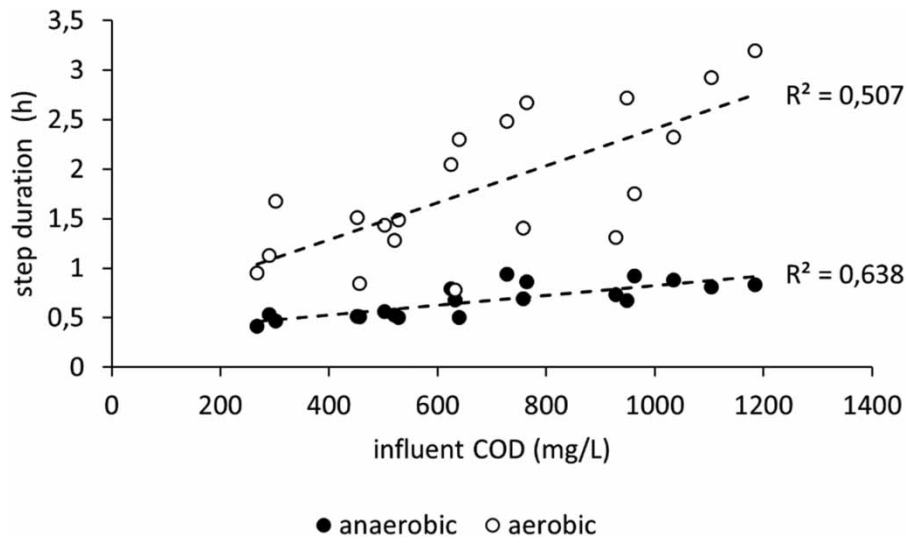

Figure 4 | Relationship between the duration of the anaerobic and aerobic reaction steps and the influent COD concentration in SBR-DYN.

50 min (Figure 5). Compared to the fixed total cycle time of SBR-STA, 6 h, this represents a significant time saving of 32%. The shorter cycle time in SBR-DYN means that the same amount of wastewater could be treated in a shorter time, resulting in a significantly higher loading rate in SBR-DYN, as shown in Figure 6. The average sludge loading rate, of food to mass ratio (F/M), in SBR-DYN was 42% higher than in SBR-STA ($p < 0.0005$, Table 2).

Table 2 shows the difference in the reactor performance parameters between both reactors. The effluent COD and PO_4-P concentrations were well below the Flemish discharge limits for surface water (125 and 2 mg L^{-1}, respectively). We should mention that, although the total phosphorus concentration (TP) was not measured, it is expected to be equally low as the average effluent suspended solids concentrations was below 10 mg L^{-1} for both reactors (data not shown). There was no statistical difference in PO_4-P removal efficiency between SBR-STA and SBR-DYN. In contrast, the COD removal efficiency was statistically higher in SBR-DYN. No clear reason for this difference was found, but more importantly, it is operationally not significant, as both the COD and PO_4-P removal efficiencies are high, and in range with values reported in previous works for AGS and conventional SBR systems treating dairy wastewater (Arrojo *et al.* 2004; Kushwaha *et al.* 2011; Bumbac *et al.* 2015;

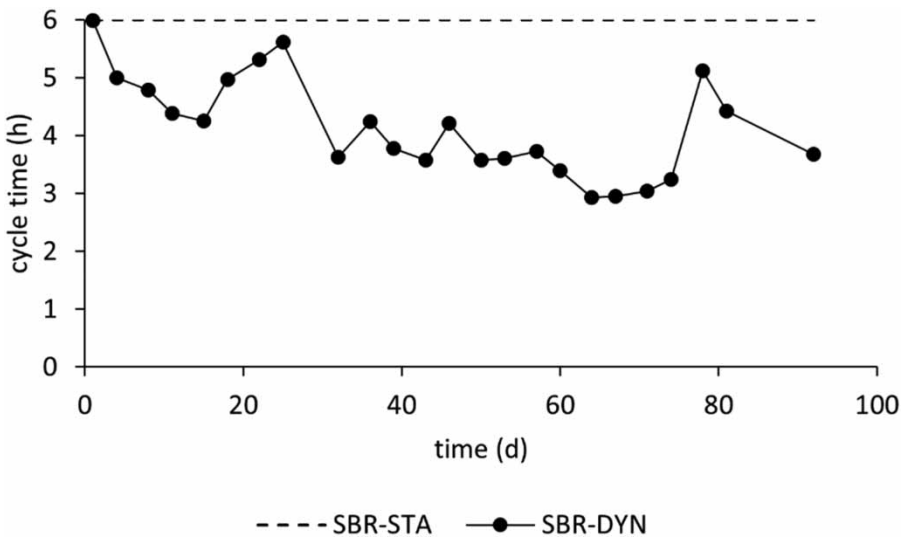

Figure 5 | Total duration of the SBR cycle in SBR-STA and SBR-DYN.

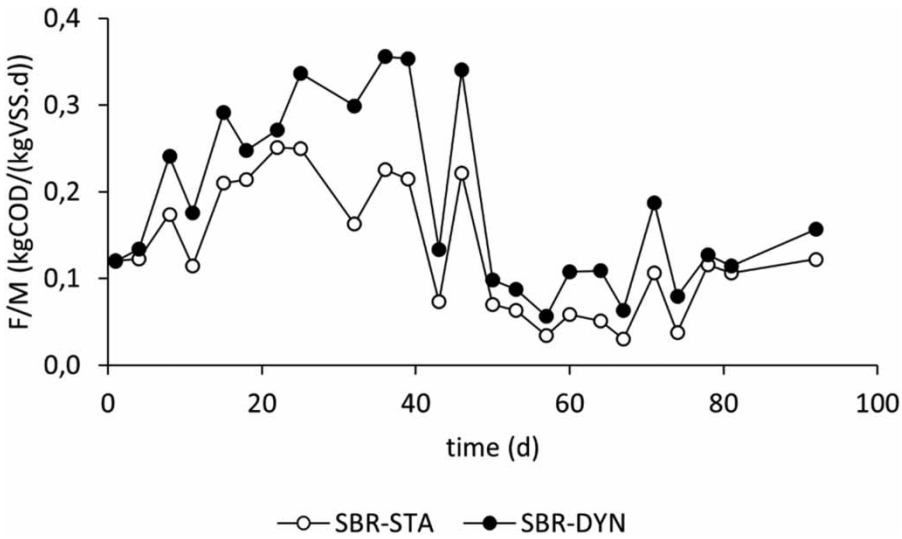

Figure 6 | Sludge loading rate (F/M ratio) in SBR-STA and SBR-DYN.

Table 2 | Average reactor performance parameters for SBR-DYN and SBR-STA, and indication of the significance of statistical differences

Parameter	Unit	SBR-DYN	SBR-STA	Signif.
Effluent COD	mg L^{-1}	28.6 ± 8.5	39.3 ± 9.4	***
COD removal	%	96 ± 3	94 ± 4	***
Effluent PO_4-P	mg L^{-1}	0.7 ± 0.4	0.6 ± 0.4	–
PO_4-P removal	%	94 ± 4	95 ± 3	–
OLR	gCOD $(m^3\ d)^{-1}$	430 ± 193	300 ± 145	***
F/M ratio	kgCOD (kgVSS $d)^{-1}$	0.19 ± 0.10	0.13 ± 0.07	***
SVI10	mL g^{-1}	75 ± 15	80 ± 14	–
SVI30	mL g^{-1}	52 ± 10	57 ± 8	*
SVI10/SVI30	–	1.43 ± 0.06	1.40 ± 0.08	–
DV50	μm	271 ± 68	229 ± 38	***
ALE content	%	27 ± 8	21 ± 7	*

–, not significant. *$p < 0.05$, **$p < 0.005$, ***$p < 0.0005$.

Meunier *et al.* 2016). With respect to N, full NH_4-N removal and almost complete N removal were observed in both reactors (results not shown).

Sludge characteristics and granulation

The average MLVSS concentration was similar in both reactors, at 2.5 ± 0.5 g L^{-1} and did not show any remarkable evolution (results not shown). The initial SVI10 and SVI30 of the seed sludge were about 112 and 75 mL g^{-1}, respectively, indicating well settling sludge. The sludge settling properties improved for both reactors during the course of the experiment, resulting in slightly lower SVI30 values in SBR-DYN ($p < 0.05$, Table 2). The SVI10/SVI30 ratio also improved, but remained well above the value of 1.0 that defines granular sludge, suggesting that full granulation was not achieved. The microscopy analyses showed that the seed sludge was fully floccular with an irregular shape (Figure 7). Within about 30 days, the morphology of the sludge evolved into larger, more dense, and better delineated aggregates. This was confirmed by the evolution of the sludge particle size (DV50). The seed sludge had a DV50 value of 158 μm, which increased to 343 and 271 μm in SBR-DYN and SBR-STA, respectively. The average DV50 of the sludge particle value was significantly higher in SBR-DYN ($p < 0.0005$, Table 2). The average ALE content was also higher in SBR-DYN, confirming the higher degree of granulation. The formation of larger granules in SBR-DYN can probably be explained by the higher organic loading rate (OLR) in SBR-DYN resulting from the shorter cycling time (Iorhemen & Liu 2021).

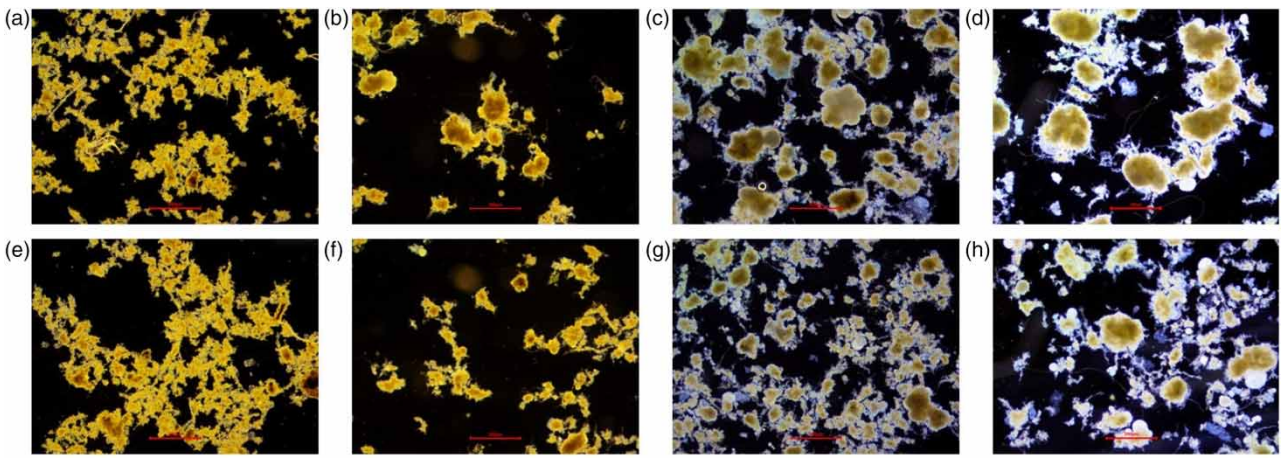

Figure 7 | Microscopy images of the sludge in SBR-DYN (a, b, c, and d) and SBR-STA (e, f, g, and h) on day 1, 33, 57, and 86. The red bar represents 500 μm.

Although granular sludge was clearly present in both reactors (Figure 7), full granulation was not obtained, and flocks were still present at the end. This hybrid floccular-granular sludge morphology was observed previously in AGS reactors treating real industrial wastewater (De Vleeschauwer *et al.* 2021; Caluwé *et al.* 2022) and can be explained by the granulation strategy applied. The main granulation driver applied in the present study was the implementation of an anaerobic feast/aerobic famine reactor operation. This reactor operation leads to the enrichment of slow-growing PAO and/or GAO that first store COD (during the anaerobic feast phase) and then consume the stored COD (during the aerobic famine phase). This strategy relates to the so-called microbial selection approach which is considered to be a main granulation mechanism (van Dijk *et al.* 2022). However, to achieve full granulation, additional mechanisms may have to be applied. These mechanisms are physical (or hydraulic) selection by selectively wasting the bad settling floccular sludge fraction, and selective feeding of the larger granule by plug-flow feeding from the bottom of the reactor. In the present study, no selective sludge wasting was applied and the influent was pulse fed into the completely mixed reactor, making microbial selection the only mechanism used. Although specific microbial analyses were not performed, the observed P release and P uptake dynamics clearly indicate PAO activity in the reactors. The average molar P release to C uptake ratio Pmol $Cmol^{-1}$ was 0.34. This ratio is lower than the value of approximately 0.5 found in fully enriched PAO systems, indicating that besides PAO also GAO were enriched in the AGS reactors (López-Vázquez *et al.* 2007; Weissbrodt *et al.* 2014). As mentioned above, both PAO and GAO are key organisms in aerobic granulation (Haaksman *et al.* 2023).

CONCLUSIONS

The current study showed, for the first time, the successful application of a sensor-based dynamic control strategy in AGS performing EBPR from real industrial wastewater. The control strategy uses common, robust, and low-cost sensors such as DO and electrical conductivity to adapt the duration of the aerobic and anaerobic reaction steps depending on the variable nature of the influent wastewater and the activity of the (granular) activated sludge. This results in a dynamic reactor operation with significant efficiency gains in the AGS process, such as lower cycle times and higher sludge loading rates without impairing the effluent quality nor the sludge properties. These results also extend the existing potential of indirect control strategies to full biological N and P removal processes, which may be of great assistance to the operators and designers of industrial installations for treatment optimization. Finally, the current study also demonstrated stable EBPR from variable dairy wastewater, holding great promise for the application of this sustainable P removal technology in industry.

ACKNOWLEDGEMENT

This work was financed by the Industrial Research Fund (IOF) of the University of Antwerp.

DATA AVAILABILITY STATEMENT

All relevant data are included in the paper or its Supplementary Information.

CONFLICT OF INTEREST

The authors declare there is no conflict.

REFERENCES

Aguado, D., Montoya, T., Ferrer, J. & Seco, A. 2006 Relating ions concentration variations to conductivity variations in a sequencing batch reactor operated for enhanced biological phosphorus removal. *Environmental Modelling & Software* **21**, 845–851. https://doi.org/10.1016/j.envsoft.2005.03.004.

Ahn, C. H. & Park, J. K. 2008 Critical factors affecting biological phosphorus removal in dairy wastewater treatment plants. *KSCE Journal of Civil Engineering* **12**, 99–107. https://doi.org/10.1007/s12205-008-0099-8.

APHA 1998 *Standard Methods for the Examination of Water and Wastewater*, 20th edn. American Public Health Association, American Water Works Association and Water Environmental Federation, Washington, DC, USA.

Arrojo, B., Mosquera-Corral, A., Garrido, J. M. & Méndez, R. 2004 Aerobic granulation with industrial wastewater in sequencing batch reactors. *Water Research* **38**, 3389–3399. https://doi.org/10.1016/j.watres.2004.05.002.

Bumbac, C., Ionescu, I. A., Tiron, O. & Badescu, V. R. 2015 Continuous flow aerobic granular sludge reactor for dairy wastewater treatment. *Water Science and Technology* **71**, 440–445. https://doi.org/10.2166/wst.2015.007.

Caluwé, M., Dobbeleers, T., D'aes, J., Miele, S., Akkermans, V., Daens, D., Geuens, L., Kiekens, F., Blust, R. & Dries, J. 2017 Formation of aerobic granular sludge during the treatment of petrochemical wastewater. *Bioresource Technology* **238**, 559–567. https://doi.org/10.1016/j.biortech.2017.04.068.

Caluwé, M., Goossens, K., Seguel Suazo, K., Tsertou, E. & Dries, J. 2022 Granulation strategies applied to industrial wastewater treatment: From lab to full-scale. *Water Science and Technology* **85**, 2761–2771. https://doi.org/10.2166/wst.2022.129.

Campo, R., Sguanci, S., Caffaz, S., Mazzoli, L., Ramazzotti, M., Lubello, C. & Lotti, T. 2020 Efficient carbon, nitrogen and phosphorus removal from low C/N real domestic wastewater with aerobic granular sludge. *Bioresource Technology* **305**, 122961. https://doi.org/10.1016/j.biortech.2020.122961.

Cornelissen, R., Van Dyck, T., Dries, J., Ockier, P., Smets, I., Van Den Broeck, R., Van Hulle, S. & Feyaerts, M. 2018 Application of online instrumentation in industrial wastewater treatment plants – A survey in Flanders, Belgium. *Water Science and Technology* **78**, 957–967. https://doi.org/10.2166/wst.2018.375.

De Kreuk, M. K. & Van Loosdrecht, M. C. M. 2004 Selection of slow growing organisms as a means for improving aerobic granular sludge stability. *Water Science and Technology* **49**, 9–17. https://doi.org/10.2166/wst.2004.0792.

De Vleeschauwer, F., Caluwé, M., Dobbeleers, T., Stes, H., Dockx, L., Kiekens, F., D'aes, J., Copot, C. & Dries, J. 2019 Performance and stability of a dynamically controlled EBPR anaerobic/aerobic granular sludge reactor. *Bioresource Technology* **280**, 151–157. https://doi.org/10.1016/j.biortech.2019.02.052.

De Vleeschauwer, F., Caluwé, M., Dobbeleers, T., Stes, H., Dockx, L., Kiekens, F., Copot, C. & Dries, J. 2021 A dynamically controlled anaerobic/aerobic granular sludge reactor efficiently treats brewery/bottling wastewater. *Water Science and Technology* **84**, 3515–3527. https://doi.org/10.2166/wst.2021.470.

Diaz, R., Mackey, B., Chadalavada, S., Kainthola, J., Heck, P. & Goel, R. 2022 Enhanced Bio-P removal: Past, present, and future – A comprehensive review. *Chemosphere* **309**, 136518. https://doi.org/10.1016/j.chemosphere.2022.136518.

Dobbeleers, T., Daens, D., Miele, S., D'aes, J., Caluwé, M., Geuens, L. & Dries, J. 2017 Performance of aerobic nitrite granules treating an anaerobic pre-treated wastewater originating from the potato industry. *Bioresource Technology* **226**, 211–219. https://doi.org/10.1016/j.biortech.2016.11.117.

Dockx, L., Caluwé, M., De Vleeschauwer, F., Dobbeleers, T. & Dries, J. 2021 Impact of the substrate composition on enhanced biological phosphorus removal during formation of aerobic granular sludge. *Bioresource Technology* **337**, 125482. https://doi.org/10.1016/j.biortech.2021.125482.

Dries, J. 2016 Dynamic control of nutrient-removal from industrial wastewater in a sequencing batch reactor, using common and low-cost online sensors. *Water Science and Technology* **73**, 740–745. https://doi.org/10.2166/wst.2015.553.

Felz, S., Al-Zuhairy, S., Aarstad, O. A., Van Loosdrecht, M. C. M. & Lin, Y. M. 2016 Extraction of structural extracellular polymeric substances from aerobic granular sludge. *JoVE,* 54534. https://doi.org/10.3791/54534.

Franca, R. D. G., Pinheiro, H. M., Van Loosdrecht, M. C. M. & Lourenço, N. D. 2018 Stability of aerobic granules during long-term bioreactor operation. *Biotechnology Advances* **36**, 228–246. https://doi.org/10.1016/j.biotechadv.2017.11.005.

Haaksman, V. A., Mirghorayshi, M., Van Loosdrecht, M. C. M. & Pronk, M. 2020 Impact of aerobic availability of readily biodegradable COD on morphological stability of aerobic granular sludge. *Water Research* **187**, 116402. https://doi.org/10.1016/j.watres.2020.116402.

Haaksman, V. A., Schouteren, M., Van Loosdrecht, M. C. M. & Pronk, M. 2023 Impact of the anaerobic feeding mode on substrate distribution in aerobic granular sludge. *Water Research* **233**, 119803. https://doi.org/10.1016/j.watres.2023.119803.

Iorhemen, O. T. & Liu, Y. 2021 Effect of feeding strategy and organic loading rate on the formation and stability of aerobic granular sludge. *Journal of Water Process Engineering* **39**, 101709. https://doi.org/10.1016/j.jwpe.2020.101709.

Izadi, P., Izadi, P. & Eldyasti, A. 2020 Design, operation and technology configurations for enhanced biological phosphorus removal (EBPR) process: A review. *Reviews in Environmental Science and Biotechnology* **19**, 561–593. https://doi.org/10.1007/s11157-020-09538-w.

Kishida, N., Tsuneda, S., Sakakibara, Y., Kim, J. H. & Sudo, R. 2008 Real-time control strategy for simultaneous nitrogen and phosphorus removal using aerobic granular sludge. *Water Science and Technology* **58**, 445–450. https://doi.org/10.2166/wst.2008.410.

Kolev Slavov, A. 2017 Dairy wastewaters – General characteristics and treatment possibilities – A review. *Food Technology and Biotechnology* **55**. https://doi.org/10.17113/ftb.55.01.17.4520.

Kushwaha, J. P., Srivastava, V. C. & Mall, I. D. 2011 An overview of various technologies for the treatment of dairy wastewaters. *Critical Reviews in Food Science and Nutrition* **51**, 442–452. https://doi.org/10.1080/10408391003663879.

López-Vázquez, C. M., Hooijmans, C. M., Brdjanovic, D., Gijzen, H. J. & Van Loosdrecht, M. C. M. 2007 A practical method for quantification of phosphorus- and glycogen-accumulating organism populations in activated sludge systems. *Water Environment Research* **79**, 2487–2498. https://doi.org/10.2175/106143007X220798.

Marsili-Libelli, S. 2006 Control of SBR switching by fuzzy pattern recognition. *Water Research* **40**, 1095–1107. https://doi.org/10.1016/j.watres.2006.01.011.

Maurer, M. & Gujer, W. 1995 Monitoring of microbial phosphorus release in batch experiments using electric conductivity. *Water Research* **29**, 2613–2617. https://doi.org/10.1016/0043-1354(95)00146-C.

Meunier, C., Henriet, O., Schoonbroodt, B., Boeur, J.-M., Mahillon, J. & Henry, P. 2016 Influence of feeding pattern and hydraulic selection pressure to control filamentous bulking in biological treatment of dairy wastewaters. *Bioresource Technology* **221**, 300–309. https://doi.org/10.1016/j.biortech.2016.09.052.

Olsson, G. 2012 ICA and me – A subjective review. *Water Research* **46**, 1585–1624. https://doi.org/10.1016/j.watres.2011.12.054.

Ribeiro, R., Von Atzingen, G. V., Lima, F., Okamoto, V. H. T., Arce, A. I. C., Tomamso, G. & Da Costa, E. J. X. 2017 Real-time control system based on the values of derivative of the redox potential aiming nitrogen removal in a sequencing batch reactor applied in treating dairy wastewater. *Water, Air, & Soil Pollution* **228**, 231. https://doi.org/10.1007/s11270-017-3401-x.

Schambeck, C. M., Girbal-Neuhauser, E., Böni, L., Fischer, P., Bessière, Y., Paul, E., Da Costa, R. H. R. & Derlon, N. 2020 Chemical and physical properties of alginate-like exopolymers of aerobic granules and flocs produced from different wastewaters. *Bioresource Technology* **312**, 123632. https://doi.org/10.1016/j.biortech.2020.123632.

Schwarzenbeck, N., Borges, J. M. & Wilderer, P. A. 2005 Treatment of dairy effluents in an aerobic granular sludge sequencing batch reactor. *Applied Microbiology and Biotechnology* **66**, 711–718. https://doi.org/10.1007/s00253-004-1748-6.

Silva, J. F., Silva, J. R., Santos, A. D., Vicente, C., Dries, J. & Castro, L. M. 2023 Continuous-flow aerobic granular sludge treatment of dairy wastewater. *Water* **15**, 1066. https://doi.org/10.3390/w15061066.

van Dijk, E. J. H., Haaksman, V. A., van Loosdrecht, M. C. M. & Pronk, M. 2022 On the mechanisms for aerobic granulation – Model based evaluation. *Water Research* **216**, 118365. https://doi.org/10.1016/j.watres.2022.118365.

Weissbrodt, D. G., Maillard, J., Brovelli, A., Chabrelie, A., May, J. & Holliger, C. 2014 Multilevel correlations in the biological phosphorus removal process: From bacterial enrichment to conductivity-based metabolic batch tests and polyphosphatase assays: Multilevel correlations in the EBPR process. *Biotechnology and Bioengineering* **111**, 2421–2435. https://doi.org/10.1002/bit.25320.

Wichern, M., Lübken, M. & Horn, H. 2008 Optimizing sequencing batch reactor (SBR) reactor operation for treatment of dairy wastewater with aerobic granular sludge. *Water Science and Technology* **58**, 1199–1206. https://doi.org/10.2166/wst.2008.486.

Yang, Q., Gu, S., Peng, Y., Wang, S. & Liu, X. 2010 Progress in the development of control strategies for the SBR process. *CLEAN – Soil, Air, Water* **38**, 732–749. https://doi.org/10.1002/clen.201000015.

Zhang, W., Wei, S. P., Winkler, M. K. H. & Mueller, A. V. 2022 Design of a soft sensor for monitoring phosphorous uptake in an EBPR process. *ACS ES&T Engineering* **2**, 1847–1856. https://doi.org/10.1021/acsestengg.2c00090.

First received 11 November 2022; accepted in revised form 3 November 2023. Available online 14 November 2023